Nonlinear Attitude Control of Flexible Spacecraft With Scissored Pairs of Control Moment Gyros

Jixiang Fan
Department of Control Science and Engineering,
Harbin Institute of Technology,
Mailbox327, Harbin, China;
Department of Electronic Engineering,
Harbin Normal University,
Harbin, China
e-mail: hwfjx@yahoo.com.cn

Di Zhou
Department of Control Science and Engineering,
Harbin Institute of Technology,
Mailbox327, Harbin, China
e-mail: zhoud@hit.edu.cn

Dynamic equations describing the attitude motion of flexible spacecraft with scissored pairs of control moment gyroscopes are established. A nonlinear controller is designed to drive the flexible spacecraft to implement three-axis large-angle attitude maneuvers with the vibration suppression. Singularity analysis for three orthogonally mounted scissored pairs of control moment gyros shows that there exists no internal singularity in this configuration. A new pseudo-inverse steering law is designed based on the synchronization of gimbal angles of the twin gyros in each pair. To improve the synchronization performance, an adaptive nonlinear feedback controller is designed for each pairs of control moment gyros by using the stability theory of Lyapunov. Simulation results are provided to show the validity of the controllers and the steering law. [DOI: 10.1115/1.4006368]

1 Introduction

Control of flexible spacecraft usually requires a controller to provide a control effort for targeting or station-keeping with the simultaneous vibration suppression. Control moment gyros (CMGs) have been used effectively for these tasks [1,2], essentially because of their large momentum-exchange capability and no need of fuel expending. As a redundant CMG cluster, pyramid-type CMG system is normally used for full three-axis control of a spacecraft. However, one of the principal difficulties in using this CMG cluster is the well-known singularity problem in which no control torque is generated for the commanded control torque along a certain direction. As evidenced in Refs. [1–4], many researchers have been focusing on the development of singularity-avoidance steering logics; nevertheless, these approaches usually produce torque errors during the escaping from singular states.

Analysis has shown that the parallel-type CMGs system has a significant ability to avoid singularity [5]. Thus, a pair of CMGs is sometimes configured into a scissor which maintains equal-magnitude and opposite-sign gamble angles for two CMGs with parallel gamble axes (see Fig. 1). A scissored pair of CMGs, like any array of CMGs, provides attitude control torque via momentum exchange with the body on which it is mounted. Most researches with this device as actuators are focused on the single-axis attitude control of the spacecraft. The Skylab-ear Astronaut Maneuvering Research Vehicle used scissored pairs for single-axis maneuver control [6]. Japanese satellite called Astro-G also employed two scissored pairs for two-degrees of freedom rest-to-rest rotational maneuvers [7]. In this brief, we study the three-axis large-angle rotational motion control of flexible spacecraft with three orthogonally mounted scissored pairs of CMGs (shown in Fig. 2). A controller is designed to ensure a rapid attitude maneuver of the spacecraft while suppressing the vibration of flexible appendages. Moreover, the singularity of the system consisting of the three orthogonally mounted scissored pairs of CMGs is analyzed. Based on the analysis, a new pseudo-inverse steering law is proposed. To improve the synchronization performance of the independent scissored pair, an adaptive controller is designed for each pair of CMGs.

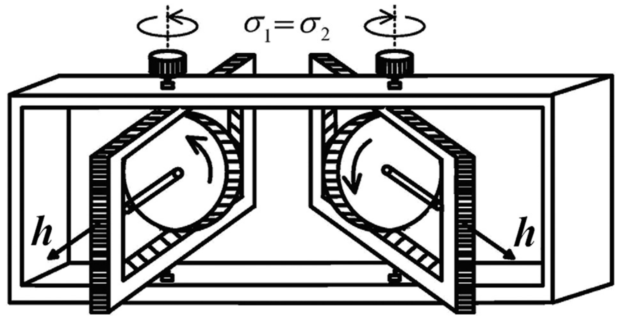

Fig. 1 Configuration of scissored pair of CMGs

2 Dynamic Modeling and Attitude Controller Design of Flexible Spacecraft

2.1 Kinematic Equations. The kinematics are parameterized by means of the unitary quaternions q_0, $\boldsymbol{q}$ [8] with $\boldsymbol{q} = [q_1 \quad q_2 \quad q_3]^T$, where $q_0 = \cos\Phi/2$, $q_i = \varepsilon_i \sin\Phi/2$, $(i = 1, 2, 3)$ subject to the constraint $\sum_{i=0}^{3} q_i^2 = 1$. Herein, Φ denotes the rotation angle of the spacecraft's main body about the Euler's axis, which is determined by the unitary vector $\boldsymbol{\varepsilon} = [\varepsilon_1 \quad \varepsilon_2 \quad \varepsilon_3]^T$. Then, the kinematic equations take the form

$$\begin{bmatrix} \dot{q}_0 \\ \dot{\boldsymbol{q}} \end{bmatrix} = \frac{1}{2}\begin{bmatrix} -\boldsymbol{q}^T \\ R(\boldsymbol{q}) \end{bmatrix}\boldsymbol{\omega} \tag{1}$$

where $\boldsymbol{\omega} = [\omega_x \quad \omega_y \quad \omega_z]^T$ is the angular velocity of the rigidified spacecraft, and

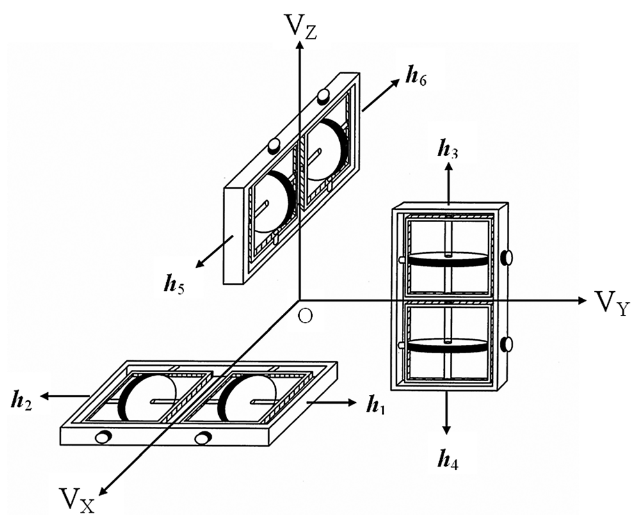

Fig. 2 Configuration of three orthogonally mounted scissored pairs of CMGs

Contributed by the Dynamic Systems Division of ASME for publication in the Journal of Dynamic Systems, Measurement and Control. Manuscript received May 18, 2010; final manuscript received February 15, 2012; published online June 5, 2012. Assoc. Editor: Rama K. Yedavalli.

$$R(\boldsymbol{q}) = \begin{bmatrix} q_0 & -q_3 & q_2 \\ q_3 & q_0 & -q_1 \\ -q_2 & q_1 & q_0 \end{bmatrix}$$

For any vector $\boldsymbol{x} = [x_1 \quad x_2 \quad x_3]^T$, $\tilde{\boldsymbol{x}}$ represents the skew symmetric cross product matrix.

2.2 Dynamic Equations. The total angular momentum of the flexible spacecraft can be written as

$$\boldsymbol{\xi} = \boldsymbol{J}_b\boldsymbol{\omega} + \boldsymbol{H} + \boldsymbol{\delta}^T\dot{\boldsymbol{\eta}} \tag{2}$$

where $\boldsymbol{J}_b$ is the symmetric inertia matrix of the spacecraft's main body, $\boldsymbol{\delta}$ is the coupling matrix between the elastic and the rigid structures, $\boldsymbol{\eta}$ is the modal coordinate vector, and $\boldsymbol{H} = \sum_{i=1}^{6} \boldsymbol{C}_i^T(\boldsymbol{J}_g\boldsymbol{C}_i\boldsymbol{\omega} + \boldsymbol{J}_g\dot{\boldsymbol{\sigma}}_i + \boldsymbol{h})$ is the angular moment of the three scissored pairs of CMGs system, where $\boldsymbol{C}_i$ is a direction cosine matrix orienting the gimbal frame with respect to the body frame, $\boldsymbol{J}_g$ is the symmetric inertia matrix of each gyro, $\dot{\boldsymbol{\sigma}}_i$ is the gimbal angular velocity vector of the ith CMG, and $\boldsymbol{h}$ is the rotor angular momentum of each gyro.

By the Euler's theorem, the hypothesis of small elastic deformations [8] and the neglect of $\boldsymbol{J}_g$, the dynamic equations can be obtained as follows:

$$\boldsymbol{J}_b\dot{\boldsymbol{\omega}} + \boldsymbol{\delta}^T\ddot{\boldsymbol{\eta}} = -\boldsymbol{\omega} \times (\boldsymbol{J}_b\boldsymbol{\omega} + \boldsymbol{H}_c + \boldsymbol{\delta}^T\dot{\boldsymbol{\eta}}) - \boldsymbol{D}\dot{\boldsymbol{\sigma}} \tag{3a}$$

$$\ddot{\boldsymbol{\eta}} + \boldsymbol{C}\dot{\boldsymbol{\eta}} + \boldsymbol{K}\boldsymbol{\eta} = -\boldsymbol{\delta}\dot{\boldsymbol{\omega}} \tag{3b}$$

where $\boldsymbol{H}_c = \sum_{i=1}^{6} \boldsymbol{C}_i^T\boldsymbol{h}$. $\boldsymbol{C} = \mathrm{diag}\{2\zeta_i\omega_{ni}, i = 1, \ldots, N\}$ and $\boldsymbol{K} = \mathrm{diag}\{\omega_{ni}^2, i = 1, \ldots, N\}$ are the damping and stiffness matrices, respectively, where ω_{ni} is the natural frequency and ζ_i is the associated damping of the ith mode. In Eq. (3a), $\boldsymbol{D}\dot{\boldsymbol{\sigma}} = \sum_{i=1}^{6} \boldsymbol{C}_i^T\dot{\tilde{\boldsymbol{\sigma}}}_i\boldsymbol{h}$ is the output torque of the CMG array. Let

$$\boldsymbol{u}_r = \boldsymbol{D}\dot{\boldsymbol{\sigma}} \tag{4}$$

The total velocities of the flexible appendages $\boldsymbol{\psi} = \boldsymbol{\delta}\boldsymbol{\omega} + \dot{\boldsymbol{\eta}}$ are introduced as new variables, dynamic equation (3) thus can be written as

$$\dot{\boldsymbol{\omega}} = -\boldsymbol{J}_m^{-1}[\boldsymbol{\omega} \times (\boldsymbol{J}_b\boldsymbol{\omega} + \boldsymbol{H}_c + \boldsymbol{\delta}^T\dot{\boldsymbol{\eta}}) - \boldsymbol{\delta}^T(\boldsymbol{C}\boldsymbol{\psi} + \boldsymbol{K}\boldsymbol{\eta} - \boldsymbol{C}\boldsymbol{\delta}\boldsymbol{\omega}) + \boldsymbol{u}_r] \tag{5a}$$

$$\dot{\boldsymbol{\eta}} = \boldsymbol{\psi} - \boldsymbol{\delta}\boldsymbol{\omega} \tag{5b}$$

$$\dot{\boldsymbol{\psi}} = -\boldsymbol{C}\boldsymbol{\psi} - \boldsymbol{K}\boldsymbol{\eta} + \boldsymbol{C}\boldsymbol{\delta}\boldsymbol{\omega} \tag{5c}$$

where $\boldsymbol{J}_m = \boldsymbol{J}_b - \boldsymbol{\delta}^T\boldsymbol{\delta}$.

2.3 Controller Design. For the attitude maneuvers of flexible spacecraft, the desired states are $[q_{0r}, \boldsymbol{q}_r] = [1, \boldsymbol{0}]$ and $\boldsymbol{\omega}_r = \boldsymbol{0}$. The final $\boldsymbol{\sigma}$ is free. Let $\hat{\boldsymbol{\eta}}$ and $\hat{\boldsymbol{\psi}}$ denote the estimates of modal variables, and $\boldsymbol{e}_\eta = \boldsymbol{\eta} - \hat{\boldsymbol{\eta}}$ and $\boldsymbol{e}_\psi = \boldsymbol{\psi} - \hat{\boldsymbol{\psi}}$ denote estimate errors. We propose the following controller and estimator

$$\boldsymbol{u}_r = \left[k_p\boldsymbol{I}, \quad \boldsymbol{\delta}^T\left\{\begin{bmatrix}\boldsymbol{K}\\ \boldsymbol{C}\end{bmatrix} - \boldsymbol{P}_1\begin{bmatrix}\boldsymbol{I}\\ -\boldsymbol{C}\end{bmatrix}\right\}^T\right]\begin{bmatrix}\boldsymbol{q}\\ \hat{\boldsymbol{\eta}}\\ \hat{\boldsymbol{\psi}}\end{bmatrix} + k_d\boldsymbol{\omega} \tag{6a}$$

$$\begin{bmatrix}\dot{\hat{\boldsymbol{\eta}}}\\ \dot{\hat{\boldsymbol{\psi}}}\end{bmatrix} = \begin{bmatrix}\boldsymbol{0} & \boldsymbol{I}\\ -\boldsymbol{K} & -\boldsymbol{C}\end{bmatrix}\begin{bmatrix}\hat{\boldsymbol{\eta}}\\ \hat{\boldsymbol{\psi}}\end{bmatrix} - \begin{bmatrix}\boldsymbol{I}\\ -\boldsymbol{C}\end{bmatrix}\boldsymbol{\delta}\boldsymbol{\omega} + \boldsymbol{P}_2^{-1}\left[\begin{bmatrix}\boldsymbol{K}\\ \boldsymbol{C}\end{bmatrix} - \boldsymbol{P}_1\begin{bmatrix}\boldsymbol{I}\\ -\boldsymbol{C}\end{bmatrix}\right]\boldsymbol{\delta}\boldsymbol{\omega} \tag{6b}$$

where $\boldsymbol{P}_i = \boldsymbol{P}_i^T (i = 1,\ 2)$ are positive-definite matrices, and k_d, k_p are positive constants.

We choose a candidate Lyapunov function as

$$V = k_p\left[(q_0 - 1)^2 + \boldsymbol{q}^T\boldsymbol{q}\right] + \frac{1}{2}\boldsymbol{\omega}^T\boldsymbol{J}_m\boldsymbol{\omega} + \frac{1}{2}\left[\boldsymbol{\eta}^T, \boldsymbol{\psi}^T\right]\boldsymbol{P}_1\begin{bmatrix}\boldsymbol{\eta}\\ \boldsymbol{\psi}\end{bmatrix} + \frac{1}{2}\left[\boldsymbol{e}_\eta^T, \boldsymbol{e}_\psi^T\right]\boldsymbol{P}_2\begin{bmatrix}\boldsymbol{e}_\eta\\ \boldsymbol{e}_\psi\end{bmatrix} \tag{7}$$

Differentiating Eq. (7) along the trajectories of Eqs. (5) and (6), and letting the matrix $\boldsymbol{P}_i$ be the solution of

$$\boldsymbol{P}_i\begin{bmatrix}\boldsymbol{0} & \boldsymbol{I}\\ -\boldsymbol{K} & -\boldsymbol{C}\end{bmatrix} + \begin{bmatrix}\boldsymbol{0} & \boldsymbol{I}\\ -\boldsymbol{K} & -\boldsymbol{C}\end{bmatrix}^T\boldsymbol{P}_i = -2\boldsymbol{Q}_i \quad i = 1, 2$$

for any given $\boldsymbol{Q}_i = \boldsymbol{Q}_i^T > \boldsymbol{0}$ result in

$$\dot{V} = -\boldsymbol{\omega}^T(k_d\boldsymbol{I} + \boldsymbol{\delta}^T\boldsymbol{C}\boldsymbol{\delta})\boldsymbol{\omega} - \left[\boldsymbol{\eta}^T, \boldsymbol{\psi}^T\right]\boldsymbol{Q}_1\begin{bmatrix}\boldsymbol{\eta}\\ \boldsymbol{\psi}\end{bmatrix} - \left[\boldsymbol{e}_\eta^T, \boldsymbol{e}_\psi^T\right]\boldsymbol{Q}_2\begin{bmatrix}\boldsymbol{e}_\eta\\ \boldsymbol{e}_\psi\end{bmatrix} \le 0 \tag{8}$$

According to the LaSalle invariance principle [9], $\boldsymbol{\omega} \to \boldsymbol{0}$, $\boldsymbol{\eta} \to \boldsymbol{0}$, $\boldsymbol{\psi} \to \boldsymbol{0}$, $\boldsymbol{\eta} \to \hat{\boldsymbol{\eta}}$, and $\boldsymbol{\psi} \to \hat{\boldsymbol{\psi}}$ as $t \to \infty$ and $\boldsymbol{q} \to \boldsymbol{0}$ along the trajectories of the controlled system $\dot{\boldsymbol{\omega}} = -\boldsymbol{J}_m^{-1}[\boldsymbol{0} + k_p\boldsymbol{q}] = \boldsymbol{0}$ as $t \to \infty$.

3 Singularity Analysis and Steering Law of Scissored Pairs of CMGs System

3.1 Singularity Analysis. In Eq. (4), $\boldsymbol{D}$ is the Jacobi matrix of the three orthogonally mounted scissored pairs of CMGs system, which can be written as

$$\boldsymbol{D} = h\begin{bmatrix} 0 & 0 & \cos\sigma_3 & \cos\sigma_4 & -\sin\sigma_5 & \sin\sigma_6 \\ -\sin\sigma_1 & \sin\sigma_2 & 0 & 0 & \cos\sigma_5 & \cos\sigma_6 \\ \cos\sigma_1 & \cos\sigma_2 & -\sin\sigma_3 & \sin\sigma_4 & 0 & 0 \end{bmatrix} \tag{9}$$

Suppose the twin gyros in each pair are completely synchronous. Hence, the condition of gimbal angles' synchronization can be written as

$$\boldsymbol{N}\dot{\boldsymbol{\sigma}} = \boldsymbol{0} \tag{10}$$

where

$$\boldsymbol{N} = \begin{bmatrix} 1 & -1 & 0 & 0 & 0 & 0 \\ 0 & 0 & 1 & -1 & 0 & 0 \\ 0 & 0 & 0 & 0 & 1 & -1 \end{bmatrix} \tag{11}$$

With Eqs. (9)–(11), the Jacobi matrix $\boldsymbol{D}$ and the rate vector of gimbal angles $\dot{\boldsymbol{\sigma}}$ can be simplified as

$$\boldsymbol{D} = 2h\begin{bmatrix} 0 & \cos\sigma_3 & 0 \\ 0 & 0 & \cos\sigma_5 \\ \cos\sigma_1 & 0 & 0 \end{bmatrix}, \quad \dot{\boldsymbol{\sigma}} = [\dot{\sigma}_1 \quad \dot{\sigma}_3 \quad \dot{\sigma}_5]^T \tag{12}$$

The singularity occurs whenever $\mathrm{rank}(\boldsymbol{D}) < 3$, i.e., $\det(\boldsymbol{D}) = 2h\cos\sigma_1\cos\sigma_3\cos\sigma_5 = 0$. Hence, there exist no internal singular states in this system and only the saturation singularity occurs whenever $\sigma_i = \pm\pi/2$.

3.2 Steering Law. The synchronization of the gimbal angles of each pair of gyros is the precondition of avoiding the internal singularity and is viewed as a constraint on designing the steering law. Then, a pseudo-inverse steering law can be derived by minimizing $\dot{\boldsymbol{\sigma}}^T\dot{\boldsymbol{\sigma}}/2$ from Eqs. (4) and (10)

$$\dot{\boldsymbol{\sigma}} = [\boldsymbol{D}^T - \boldsymbol{N}^T(\boldsymbol{N}\boldsymbol{N}^T)^{-1}\boldsymbol{N}\boldsymbol{D}^T][\boldsymbol{D}\boldsymbol{D}^T - \boldsymbol{D}\boldsymbol{N}^T(\boldsymbol{N}\boldsymbol{N}^T)^{-1}\boldsymbol{N}\boldsymbol{D}^T]^{-1}\boldsymbol{u}_r \tag{13}$$

4 Dynamic Equations and Controller Design for Scissored Pairs of CMGs

The redundant CMG system is usually selected as an actuator for 3D attitude control of the spacecraft, because its extra degrees of freedom may reduce the possibility of encountering singular states and maintain the capability of outputting 3D torque by reconfiguration if one or more CMGs are invalid. Although a constrained scissored pair has relative merits on the internal torque cancelation and the resulting power savings as compared with an independent scissored pair [10], considering the gimbal restrict of the constrained scissored pair for reconfiguration, we employ the independent scissored pair in this work. Yang et al. [11,12] investigated the synchronization control strategy of independent scissored pair, proposed a feedforward/feedback moment-gyro control method in the slewing motion control of a flexible truss arm, and applied the cross-coupling adaptive synchronization control scheme to two gyros' synchronous precession. In their article, the slewing motion control is implemented in the open loop, whereas the synchronous precession control of twin gyros is realized in the closed loop. To deal with the effect of external disturbances acting on gimbal axis, in this section, a closed loop adaptive nonlinear synchronization control law is presented.

4.1 Dynamic Equations. According to the momentum moment theorem, the dynamic equation of the ith CMG can be expressed as

$$\boldsymbol{J}_g\ddot{\boldsymbol{\sigma}}_i + \tilde{\dot{\boldsymbol{\sigma}}}_i\boldsymbol{h} + \boldsymbol{M}_i = \boldsymbol{L}_i \tag{14}$$

where $\boldsymbol{M}_i = \boldsymbol{J}_g\boldsymbol{C}_i\dot{\boldsymbol{\omega}} - \boldsymbol{J}_g\tilde{\dot{\boldsymbol{\sigma}}}_i\boldsymbol{C}_i\boldsymbol{\omega} + \boldsymbol{C}_i\tilde{\boldsymbol{\omega}}\boldsymbol{C}_i^T\boldsymbol{J}_g\boldsymbol{C}_i\boldsymbol{\omega} + \tilde{\dot{\boldsymbol{\sigma}}}_i\boldsymbol{J}_g\boldsymbol{C}_i\boldsymbol{\omega} + \boldsymbol{C}_i\tilde{\boldsymbol{\omega}}\boldsymbol{C}_i^T\boldsymbol{J}_g\dot{\boldsymbol{\sigma}}_i + \boldsymbol{C}_i\tilde{\boldsymbol{\omega}}\boldsymbol{C}_i^T\boldsymbol{h}$ and $\boldsymbol{L}_i = \boldsymbol{u}_i + \boldsymbol{d}_i$, where $\boldsymbol{u}_i$ represent the input torque vector, and $\boldsymbol{d}_i$ represent the disturbance torque vector.

Writing the vectors in Eq. (14) in the gimbal frame, we obtain $\boldsymbol{J}_g\ddot{\boldsymbol{\sigma}}_i = [0 \quad 0 \quad J_z\ddot{\sigma}_i]^T$, $\tilde{\dot{\boldsymbol{\sigma}}}_i\boldsymbol{h} = [0 \quad \dot{\sigma}_i h \quad 0]^T$, $\boldsymbol{u}_i = [0 \quad 0 \quad u_i]^T$, and $\boldsymbol{d}_i = [0 \quad 0 \quad d_i]^T$. Equation (14) thus can be rewritten as

$$\begin{cases} M_{ix} = L_{ix} \\ \dot{\sigma}_i h + M_{iy} = L_{iy} \\ J_z\ddot{\sigma}_i + M_{iz} = L_{iz} \end{cases}$$

where L_{ix} and L_{iy} are the two components of the reaction torque and $L_{iz} = u_i + d_i$ is the sum of the control torque and the disturbance torque.

4.2 Controller Design. With the first scissored pair of CMGs as an example, we define the gimbal angle tracking errors $e_1 = \sigma_1 - \sigma_{1r}$, $e_2 = \sigma_2 - \sigma_{2r}$, where σ_{ir} $(i = 1, 2)$ are the desired gimbal angles. By the steering law (13), we can obtain the desired angular velocities of gyros 1 and 2, i.e., $\dot{\sigma}_{ir}$ $(i = 1, 2)$. Then integrating $\dot{\sigma}_{ir}$ with zero initial values gives σ_{ir}. In the presence of disturbances d_1 and d_2, the synchronization error defined by the difference of the two gimbal angles, i.e., $\varepsilon = e_1 - e_2$, must be suppressed by a feedback strategy. Introducing the integral of the synchronization error into the system as a new independent variable, we choose state variables of the synchronization control system as $x_1 = \int_0^t \varepsilon dt$, $x_2 = e_1$, $x_3 = e_2$, $x_4 = \dot{e}_1$, and $x_5 = \dot{e}_2$. The state equations are then given by

$$\dot{\boldsymbol{X}} = \boldsymbol{A}\boldsymbol{X} + \boldsymbol{B}\boldsymbol{u} + [\boldsymbol{0} \quad \boldsymbol{\Phi}]^T + \boldsymbol{B}\boldsymbol{d} \tag{15}$$

where $\boldsymbol{X} = [x_1 \quad x_2 \quad x_3 \quad x_4 \quad x_5]^T$, $\boldsymbol{u} = [u_1 \quad u_2]^T$, $\boldsymbol{d} = [d_1 \quad d_2]^T$, $\boldsymbol{A} = \begin{bmatrix} \boldsymbol{A}_1 & \boldsymbol{A}_2 \\ \boldsymbol{0} & \boldsymbol{0} \end{bmatrix}$, $\boldsymbol{B} = \begin{bmatrix} \boldsymbol{0} \\ \boldsymbol{\Gamma} \end{bmatrix}$,

$$\boldsymbol{\Phi} = \begin{bmatrix} -\ddot{\sigma}_{1r} - \dfrac{M_{1z}}{J_z} \\ -\ddot{\sigma}_{2r} - \dfrac{M_{2z}}{J_z} \end{bmatrix} \quad \text{with} \quad \boldsymbol{A}_1 = \begin{bmatrix} 0 & 1 & -1 \\ 0 & 0 & 0 \\ 0 & 0 & 0 \end{bmatrix},$$

$$\boldsymbol{A}_2 = \begin{bmatrix} 0 & 0 \\ 1 & 0 \\ 0 & 1 \end{bmatrix}, \quad \boldsymbol{\Gamma} = \begin{bmatrix} 1/J_z & 0 \\ 0 & 1/J_z \end{bmatrix}$$

In an adaptive controller design, we consider canceling the influence of the constant components of d_1 and d_2. It is easy to check the controllability of the system $\dot{\boldsymbol{X}} = \boldsymbol{A}\boldsymbol{X} + \boldsymbol{B}\boldsymbol{u}$ by using the well-known controllability criterion for linear time invariant systems.

The adaptive estimate of the disturbance vector is denoted by $\hat{\boldsymbol{d}}$ and the estimate error vector is defined by $\boldsymbol{e}_d = \boldsymbol{d} - \hat{\boldsymbol{d}}$. We design the following adaptive controller for scissored pair of CMGs:

$$\boldsymbol{u} = -\boldsymbol{K}\boldsymbol{X} - \boldsymbol{\Gamma}^{-1}\boldsymbol{\Phi} - \hat{\boldsymbol{d}} \tag{16a}$$

$$\dot{\hat{\boldsymbol{d}}} = \gamma\boldsymbol{B}^T\boldsymbol{P}\boldsymbol{X} \tag{16b}$$

to ensure the global asymptotic stability of the system (15), where γ is a symmetric positive define matrix, and $\boldsymbol{K} = \boldsymbol{R}^{-1}\boldsymbol{B}^T\boldsymbol{P}$ is the feedback gain matrix. Matrix $\boldsymbol{P}$ is the solution of matrix Riccati equation $\boldsymbol{A}^T\boldsymbol{P} + \boldsymbol{P}\boldsymbol{A} - \boldsymbol{P}\boldsymbol{B}\boldsymbol{R}^{-1}\boldsymbol{B}^T\boldsymbol{P} = -\boldsymbol{Q}$, where $\boldsymbol{R}$ and $\boldsymbol{Q}$ are the given symmetric positive-definite matrices.

Construct a Lyapunov function for the system represented by Eqs. (15) and (16) as

$$V = \frac{1}{2}\boldsymbol{X}^T\boldsymbol{P}\boldsymbol{X} + \frac{1}{2}\boldsymbol{e}_d^T\gamma^{-1}\boldsymbol{e}_d \tag{17}$$

The time derivative of V along the trajectories of the system is given by

$$\dot{V} = -\frac{1}{2}\boldsymbol{X}^T\boldsymbol{Q}\boldsymbol{X} - \frac{1}{2}\boldsymbol{X}^T\boldsymbol{P}\boldsymbol{B}\boldsymbol{R}^{-1}\boldsymbol{B}^T\boldsymbol{P}\boldsymbol{X} \le -\frac{1}{2}\boldsymbol{X}^T\boldsymbol{Q}\boldsymbol{X} \le 0 \tag{18}$$

According to the Barbalat lemma [9], we know that $\boldsymbol{X}$ approaches zero asymptotically; therefore, the system has the global asymptotic stability. The first term in the controller (16a) is the linear quadratic optimal control for the system $\dot{\boldsymbol{X}} = \boldsymbol{A}\boldsymbol{X} + \boldsymbol{B}\boldsymbol{u}$, which minimizes the linear quadratic performance $\int_0^\infty (\boldsymbol{X}^T\boldsymbol{Q}\boldsymbol{X} + \boldsymbol{u}^T\boldsymbol{R}\boldsymbol{u})dt$. As a state variable, the integral of the synchronization error is independently penalized by the corresponding entry in the weighting matrix $\boldsymbol{Q}$ such that the synchronization performance may be improved.

5 Simulations

The satellite consists of a rigid main body with three scissored pairs of CMGs and a flexible appendage. The parameters of the satellite are given by

$$\boldsymbol{J}_b = \begin{bmatrix} 980 & 29 & 11.5 \\ 29 & 390 & 11.3 \\ 11.5 & 11.3 & 630 \end{bmatrix}, \quad \boldsymbol{\delta} = \begin{bmatrix} 10 & 0.5 & 0.2 \\ 0.5 & 2 & 0 \\ 0.1 & 10.9 & 0.8 \\ 1 & 0.5 & 0.5 \end{bmatrix},$$

$$\boldsymbol{J}_g = \mathrm{diag}\{0.07 \quad 0.05 \quad 0.05\}, \quad \boldsymbol{h} = [75 \quad 0 \quad 0]^T$$

For the flexible appendage, the natural frequencies of the four modes and the associated damping are given as $\omega_{n1} = 1.9$, $\omega_{n2} = 4.1$, $\omega_{n3} = 5.8$, $\omega_{n4} = 6$, and $\zeta_1 = 0.05$, $\zeta_2 = 0.04$, $\zeta_3 = 0.16$, $\zeta_4 = 0.005$. The initial attitude of the spacecraft is described by the quaternions $q_0(0) = 0.17365$, $q_1(0) = 0.91856$, $q_2(0) = -0.29544$, and $q_3(0) = 0.19696$. The initial angular velocities of the spacecraft are zero. The initial gimbal angles of

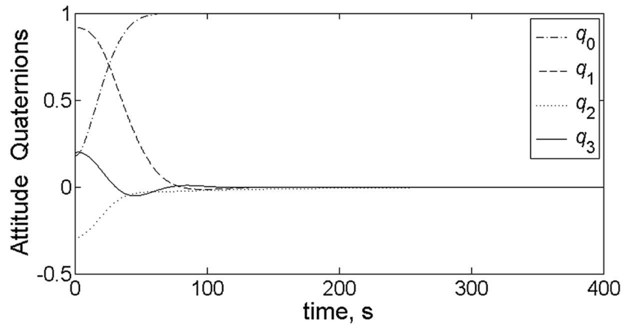

Fig. 3 Attitude quaternions

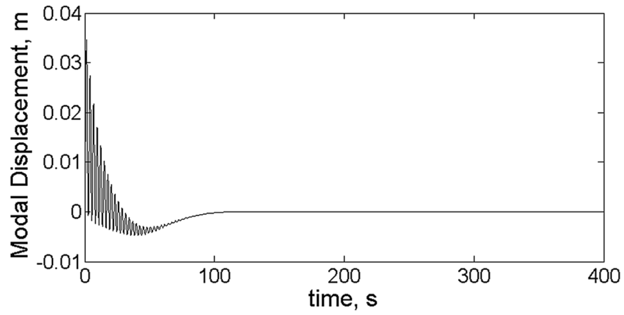

Fig. 4 Modal displacement η_1

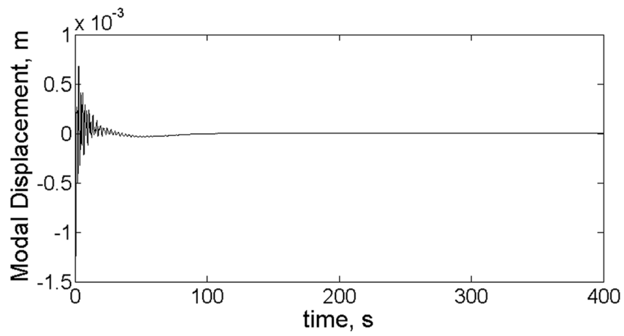

Fig. 5 Modal displacement η_2

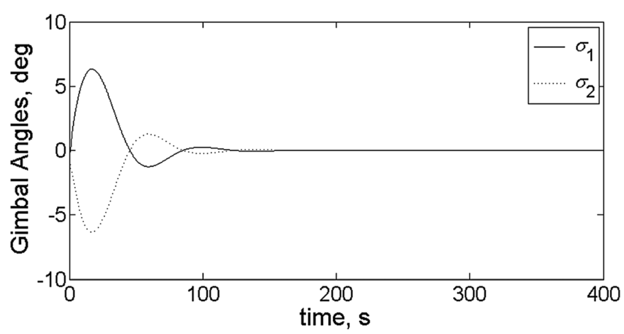

Fig. 6 Gimbal angles σ_1 and σ_2

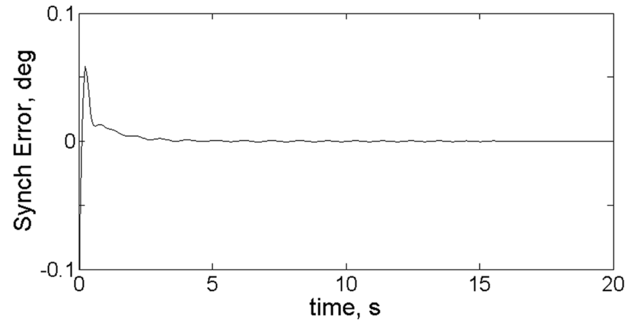

Fig. 7 Synchronization error ε_1

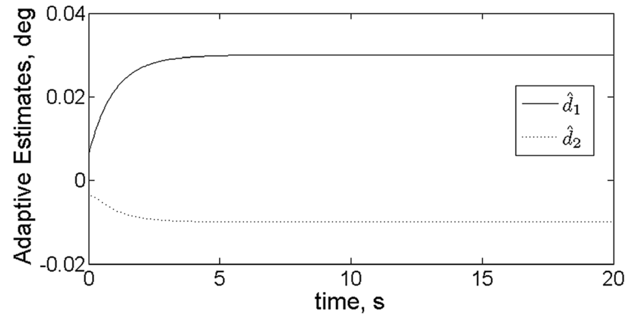

Fig. 8 Adaptive estimates $\hat{d}_1$ and $\hat{d}_2$

the gyros and their rates are zero. All initial estimates are zero. A large-angle maneuver mission is assigned to the flexible spacecraft such that its attitude is adjusted to the desired states $[q_{0r}, \boldsymbol{q}_r] = [1, \boldsymbol{0}]$ and $\boldsymbol{\omega}_r = \boldsymbol{0}$. In the mission, constant disturbances $\boldsymbol{d} = [0.03 \quad -0.01 \quad -0.02 \quad 0.01 \quad -0.04 \quad 0.04]^T$ are imposed on the gimbal axes of the CMGs system. The parameters of the attitude controller (6) are selected as $k_p = 10$, $k_d = 50$, $\boldsymbol{Q}_1 = \boldsymbol{I}$, and $\boldsymbol{Q}_2 = 2.5\boldsymbol{I}$. In the CMGs controller (16), the weighting matrices are selected as $\boldsymbol{R} = \mathrm{diag}(1 \quad 1)$, $\boldsymbol{Q} = \mathrm{diag}(10^6 \quad 10^3 \quad 10^3 \quad 10^2 \quad 10^2)$, and $\gamma = \boldsymbol{I}$, where $\boldsymbol{I}$ represents a 2×2 identity matrix. As observed, the first diagonal entry in matrix $\boldsymbol{Q}$ is larger than the others so as to emphasize the synchronization performance.

The time histories of attitude quaternions are plotted in Fig. 3. The modal displacement of the first mode and that of the second mode are plotted in Figs. 4 and 5, respectively. With the first pair of CMGs as an example, the gimbal angles of the twin gyros are plotted in Fig. 6; the synchronization error between them is plotted in Fig. 7; and the estimates for the disturbances on the two gyros are plotted in Fig. 8. As seen from Figs. 3–5, while the spacecraft performs the attitude maneuver, the vibrations of the flexible appendages are efficiently suppressed. In the attitude maneuver process, the gimbal angles of the scissored pair of CMGs are kept synchronous (see Fig. 6) and the synchronization error between them asymptotically converges to zero (see Fig. 7). Moreover, the adaptive estimates for the gyro disturbances, $\hat{d}_1$ and $\hat{d}_2$, converge to the real values of d_1 and d_2, respectively (see Fig. 8).

6 Conclusions

Dynamic equations for the attitude motion of flexible spacecraft with three scissored pairs of CMGs as actuators are presented. Based on the second method of Lyapunov, a nonlinear output-feedback controller, using the attitude quaternions and angular velocity of the spacecraft, is proposed. Simulation results show that the flexible spacecraft successfully performs large-angle attitude maneuvers while suppressing vibrations by using the controller.

The three scissored pairs of CMGs are suggested to be orthogonally mounted. Singularity analysis shows that there exist no internal singular states in such a configuration if the gimbal angles of each pair of CMGs are synchronized. As the precondition of avoiding the internal singularity, the synchronization of the gimbal angles of each pair of gyros is viewed as a constraint on designing the CMGs steering law, consequently, the new pseudo-inverse steering law for this CMGs system is proposed. To improve the synchronization performance of each pair of CMGs, we introduce the integral of synchronization error into the gyros' feedback control system as an additional state variable and then design an adaptive controller for the synchronization control system. With this adaptive controller, in the large-angle attitude maneuvers task, the synchronization error between the gimbal angles of the scissored pair of CMGs asymptotically tends to zero in the presence of external disturbance, the synchronization performance is significantly improved.

Acknowledgment

This work was supported in part by the Natural Science Foundation of China under Grant Nos. 60674102 and 61174203 and Program for New Century Excellent Talents in University (NCET-08–0153). Authors fully appreciate the financial support.

References

[1] Vadali, S. R., Oh, H.-S., and Walker, S. R., 1990, "Preferred Gimbal Angles for Single Gimbal Control Moment Gyros," J. Guid. Control Dyn., **13**(6), pp. 1090–1095.
[2] Heiberg, C. J., Bailey, D., and Wie, B., 2000, "Precision Spacecraft Pointing Using Single-Gimbal Control Moment Gyros With Disturbance," J. Guid. Control Dyn., **23**(1), pp. 77–85.
[3] Ford, K. A., and Hall, C. D., 2000, "Singular Direction Avoidance Steering for Control Moment Gyros," J. Guid. Control Dyn., **23**(4), pp. 648–656.
[4] Wie, B., Bailey, D., and Heiberg, C., 2001, "Singularity Robust Steering Logic for Redundant Single-Gimbal Control Moment Gyros," J. Guid. Control Dyn., **24**(5), pp. 865–872.
[5] Wie, B., 2004, "Singularity Analysis and Visualization for Single-Gimbal Control Moment Gyro Systems," J. Guid. Control Dyn., **27**(2), pp. 271–282.
[6] Murtagh, T. B., Whitsett, C. E., Goodwin, M. A., and Greenlee, J. E., 1974, "Automatic Control of the Skylab Astronaut Maneuvering Research Vehicle," J. Spacecr. Rockets, **11**(5), pp. 321–326.
[7] Kamiya, T., Maeda, K., Ogura, N., Sakai, S.-I., 2009, "Flexible Spacecraft Rest-to-Rest Maneuvers With CMGs Parallel Gimbal Arrangement," Proceedings of the International Conference Guidance Navigation and Control, Chicago, IL, Aug. 10–13.
[8] Di Gennaro, S., 2003, "Passive Attitude Control of Flexible Spacecraft From Quaternion Measurements," J. Optim. Theory Appl., **116**(1), pp. 41–60.
[9] Khalil, H. K., 1996, *Nonlinear Systems*, Prentice-Hall, Upper Saddle River, NJ.
[10] Brown, D., and Peck, M. A., 2008, "Scissored-Pair Control-Moment Gyros: A Mechanical Constraint Saves Power," J. Guid. Control Dyn., **31**(6), pp. 1823–1826.
[11] Yang, L. F., Mikulas, M. M., Jr., Park, K. C., and Su, R., 1995, "Slewing Maneuvers and Vibration Control of Space Structures by Feedforward/Feedback Moment-Gyro Controls," ASME J. Dyn. Syst., Meas. Control, **117**(3), pp. 343–351.
[12] Yang, L. F., and Chang, W. H., 1996, "Synchronization of Twin-Gyro Precession Under Cross-Coupled Adaptive Feedforward Control," J. Guid. Control Dyn., **19**(3), pp. 534–539.